Atmos. Chem. Phys. Discuss., https://doi.org/10.5194/acp-2018-344
Manuscript under review for journal Atmos. Chem. Phys.
Discussion started: 22 May 2018

Atmospheric Chemistry and Physics Discussions

Observing local CO_2 sources using low-cost, near-surface urban monitors

Alexis A. Shusterman[1], Jinsol Kim[2], Kaitlyn J. Lieschke[1], Catherine Newman[1], Paul J. Wooldridge[1], Ronald C. Cohen[1,2]

[1]Department of Chemistry, University of California, Berkeley, Berkeley, 94720, CA, USA
[2]Department of Earth and Planetary Science, University of California, Berkeley, Berkeley, CA, 94720, USA

Correspondence to: Ronald C. Cohen (rccohen@berkeley.edu)

Abstract. Urban carbon dioxide comprises the largest fraction of anthropogenic greenhouse gas emissions but also the most challenging monitoring, reporting, and verification (MRV) task, as numerous emission sources reside in close proximity within each topographically intricate urban dome. In attempting to better understand each individual source's contribution to the overall emission budget, there exists a large gap between activity-based emission inventories and observational constraints on integrated, regional emission estimates. Here we leverage urban CO_2 observations from the BErkeley Atmospheric CO_2 Observation Network (BEACO$_2$N) to enhance, rather than average across or cancel out, our sensitivity to these hyperlocal emission sources. We utilize a method for isolating the local component of a CO_2 signal that accentuates the observed intra-urban heterogeneity and thereby increases sensitivity to mobile emissions from specific highway segments. We demonstrate a multiple linear regression analysis technique that accounts for boundary layer and wind effects and allows for the detection of changes in traffic emissions on scale with anticipated changes in vehicle fuel economy–an unprecedented level of sensitivity for low-cost sensor technologies. The ability to represent trends of policy-relevant magnitudes with a low-cost sensor network has important implications for future applications of this approach, whether as a supplement to sparser existing reference networks or as a substitute in areas where fewer resources are available.

1 Introduction

Initiatives to curb greenhouse gas emissions and thereby reduce the extent of climate change-related damages are gaining momentum from city to global scales (United Nations, 2015). To support this effort, there is a clear need for monitoring, reporting, and verification (MRV) strategies capable of describing emission changes and attributing those changes to the relevant policy measures (Pacala et al., 2010). Currently, an estimated 70% of global CO_2 emissions are urban in origin and this fraction is expected to grow as migration to urban areas continues and intensifies with the industrialization of developing nations (United Nations, 2011). However, cities also present the largest MRV challenge in that many disparate emission sources combine with complex topography.

A considerable amount of MRV-related work has been invested in the development of activity-based emission inventories for selected metropolitan areas, such as Indianapolis (Gurney et al., 2012), Paris (Bréon et al., 2015), Los Angeles (Newman

Atmos. Chem. Phys. Discuss., https://doi.org/10.5194/acp-2018-344
Manuscript under review for journal Atmos. Chem. Phys.
Discussion started: 22 May 2018

et al., 2016), Salt Lake City (Patarasuk et al., 2016), and Toronto (Pugliese et al., 2017), as well as other inventories constructed and maintained by individual air management agencies for internal use. These inventories, when updated regularly, offer the possibility of direct source attribution without the use of computationally intense and/or heavily parameterized atmospheric transport models; they do, however, typically rely on interpolations, generalizations, or proxies to generate the necessary input activity data. The FIVE inventory developed by McDonald et al. (2014), for example, uses a representative 7 days of highway traffic flow measurements to drive the weekly cycle of CO_2 emissions from mobile sources on roads of all sizes year round. While traffic patterns as well as residential and commercial energy usage are known to vary by day of week (Harley et al., 2005), the specific timing and magnitude of these variations are likely to be heterogeneous in space and time. Mobile emission estimates constructed using an average week of highway observations therefore neglect the impact of anomalous events as well as the variety of vehicle fleets, commute practices, and congestion patterns that occur at the neighborhood level. As knowledge of emission factors and fuel efficiency grows, activity data will become one of the largest sources of uncertainty in bottom-up inventory products.

Ambient atmospheric measurements offer the opportunity to observe nuanced variations in CO_2 emission activities directly without generalizing across space and time. In order to document baseline conditions in and upcoming changes to urban greenhouse gas emissions, surface-level monitoring campaigns in cities using varied approaches are being pursued (e.g. Bréon et al., 2015; Chen et al., 2016; McKain et al., 2012; McKain et al., 2015; Shusterman et al., 2016; Turnbull et al., 2015; and Verhulst et al., 2017). These networks, typically consisting of 2–15 instruments, attempt to constrain and supplement activity-based emission inventories with observation-based estimates. Most previous work on observation-based emission estimates has focused on domain-wide emission totals over monthly to annual timescales (e.g., Kort et al., 2013). This emphasis on integrated signals has led to site selection and data analysis techniques that minimize sensitivity to local emissions, thus discarding a large portion of the information contained in the datasets collected at individual measurement sites and the differences between them (Shusterman et al., 2016; Turner et al., 2016).

We hypothesize that, if trends in the specific, small-scale CO_2 sources implicated in most mitigation strategies are to be resolved from atmospheric monitoring datasets, site-to-site heterogeneity must be sought out and retained. Here we present an initial characterization of the degree of spatial heterogeneity present in an urban monitoring dataset and offer these direct observations of intracity heterogeneities as a possible strategy for providing direct constraints on CO_2 emissions from individual sectors. We provide an initial approach to quantifying changes in the mobile sector and separating the influence of that sector from other emissions.

2 Measurements

2.1 The BErkeley Atmospheric CO_2 Observation Network

The BErkeley Atmospheric CO_2 Observation Network (BEACO$_2$N; see Shusterman et al., 2016) is an ongoing greenhouse gas and air quality monitoring campaign operating in the San Francisco Bay Area since late 2012. The current network is comprised

Atmos. Chem. Phys. Discuss., https://doi.org/10.5194/acp-2018-344
Manuscript under review for journal Atmos. Chem. Phys.
Discussion started: 22 May 2018

of ~50 "nodes" stationed on top of schools and museums at approximate 2 km intervals (Fig. 1). The nodes contain a variety of commercially available, low-cost sensor technologies: a Vaisala CarboCap GMP343 for CO_2, a Shinyei PPD42NS for particulate matter, a suite of Alphasense B4 electrochemical devices for O_3, CO, NO, and NO_2, as well as meteorological sensors for pressure, temperature, and relative humidity. Data is collected every 2–10 s and transmitted wirelessly or via an onsite Ethernet connection to a central server, where it is made publicly available in near real time. The distributed low-cost dataset is supplemented by a "supersite" at the RFS location featuring a Picarro G2401 cavity ring-down spectroscopy analyzer for CO_2, CO, and H_2O, a TSI Optical Particle Sizer 3330 for particulate matter, a ThermoFisher Scientific 42i-TL NO_x analyzer for NO and NO_2, a Teledyne 703E photometric calibrator for O_3, a Pandora spectrometer system for total column O_3 and NO_2, a Lufft CHM 15k ceilometer for cloud and aerosol layer height, as well as various instruments for meteorological measurements (i.e. a Vaisala WXT520 weather transmitter, a Campbell Scientific CS500 temperature and relative humidity probe, and a Davis Vantage Pro2 system with a Davis 6410 anemometer and Davis 6450 solar radiation sensor). This high-cost, reference-grade instrumentation serves as a high-accuracy anchor point within the network domain. Atmospheric boundary conditions are monitored by the Bay Area Air Quality Management District's Greenhouse Gas Measurement Program, which maintains its own reference instruments at four background sites to the northwest, east, southeast, and south. A description of the design, deployment, and evaluation of the BEACO$_2$N approach can be found in Shusterman et al. (2016) and Kim et al. (2017).

Here we utilize CO_2 observations from the 20 BEACO$_2$N sites operating most consistently during the summer and/or winter of 2017 (Table 1), defined as 1 June 2017 through 30 September 2017 and 1 November 2017 through 31 January 2018, respectively. The raw 2 s CO_2 concentrations are averaged to 1 min means, which are subsequently converted to bias-corrected dry air mole fractions using site-specific meteorological observations and in-network reference measurements (see Shusterman et al., 2016). The processed 1 min averages are assumed to have an uncertainty of less than ±4 ppm, or ±0.5 ppm at the hourly temporal resolution discussed most often hereafter.

2.2 Traffic Counts

Traffic count data is collected by the California Department of Transportation as part of the Caltrans Performance Measurement System (PeMS; http://pems.dot.ca.gov/). Hourly passenger vehicle flow data (in vehicles per hour) are obtained from the road monitors nearest to the relevant BEACO$_2$N site with >50% directly observed (as opposed to modeled) data and are summed across all lanes and directions. Due to limited data coverage, in some cases it is necessary to sample road monitors upstream or downstream of the desired roadway segment; here we assume the sampled traffic conditions to be reasonable approximations of those on the desired segment. The specific monitor IDs used in each analysis are given in Table 1.

3 Results & Discussion

To quantify the spatial heterogeneity present across the network, we examine the degree of correlation between every possible pairing of sites in a given season as a function of the distance between them (Figs. 2 and 3), borrowing from a similar analysis

used by McKain et al. (2012). For straightforward comparison with the McKain et al. results, we first average to 5 min resolution and allow for up to a ±3 h lag between the two time series before performing a linear regression and choosing the optimal r^2 value.

In the summer months, there appears to be some relationship between the proximity of the sites and the correlation of their observations at all hours, with higher correlations between neighboring sites decaying into more modest, but still significant, correlations at longer inter-site distances. The characteristic length scale of this correlation is 2.9 km (defined as the e-folding distance of the exponential fits in Fig. 2; 3.6 km during the day and 2.2 km at night). The winter months meanwhile exhibit lower pairwise correlations overall and shorter correlation lengths (2.4 km; 2.6 km during the day and 2.1 km at night). Some portion of the summer–winter differences may be attributable to seasonal differences in dominant wind patterns, although this effect is difficult to disentangle from the slightly different collection of sites sampled during the two seasons; the winter sample, for example, contains fewer pairs with separation lengths less than 5 km, which affects the perceived overall trend. In either season, the correlation lengths are considerably longer than the ~100 to 1000 m e-folding distances of urban pollutants derived by previous studies (e.g. Zhu et al., 2006; Beckerman et al., 2008; Choi et al., 2014), however, the correlation length observed here does validate the original choice of 2 km as the desirable inter-site separation in the design of the BEACO$_2$N instrument.

The 24 hour findings (top panels of Figs. 2 and 3) compare well to those presented by McKain et al., who also documented a decaying but nevertheless persistent correlation with increasing site separation. However, whereas McKain et al. saw very little correlation after restricting their analysis to daytime hours, even at very short (< 5 km) inter-site distances, we observe moderate to high correlations during the day. This suggests that the data record at a particular BEACO$_2$N site contains information about both local and regional emissions and transport phenomena. While the regionwide phenomena can be characterized using sparser networks of high-cost, conventional monitoring equipment, the ability to capture to local processes is unique to the high-density approach.

We posit that the true strength of a high-density, surface-level monitoring network lies in its characterization of hyperlocal phenomena unique to a given site or subset of sites. In order to directly examine signals attributable to these specific, local CO_2 emission processes, we separate each site's observations into a "regional" and "local" component. The regional component is, by definition, the same at all sites network-wide, calculated from the bottom 10th percentile of all BEACO$_2$N readings collected during the surrounding 1 h window. The bottom 10th percentile is chosen (rather than the absolute minimum) to account for measurement error (see Shusterman et al., 2016) as well as any nearfield draw down from the local biosphere; negative values in the local signals are likely attributable to some combination of these effects. While many different sites contribute to this bottom 10th percentile over the course of the data record, some sites located in close proximity to emission sources are never represented in the bottom 10th percentile and always exhibit some enhancement (i.e. a non-zero local component) over the regional background signal. The regional component is allowed to vary throughout the data record and will therefore reflect domain-wide changes in response to day of week, synoptic weather events, etc.

The diel profiles of the regional signal measured in summer and winter 2017 are shown in Fig. 2, reflecting the typical convolution of background concentrations, emission processes, and dynamics experienced across the entire BEACO$_2$N

Atmos. Chem. Phys. Discuss., https://doi.org/10.5194/acp-2018-344
Manuscript under review for journal Atmos. Chem. Phys.
Discussion started: 22 May 2018

Atmospheric Chemistry and Physics Discussions

domain. In both seasons, we see an increase in the regional signal beginning around 0400 local time (LT), followed by a decrease in concentrations at 0800 LT in the winter months and 1200 LT in the summer, and another increase in early to late afternoon depending on the season. This diurnal profile corresponds well with known patterns in traffic emissions–which are largely consistent across seasons–superimposed on diel fluctuations in boundary layer height that vary in timing and magnitude according to the season. Namely, the nighttime boundary layer in the BEACO$_2$N domain appears to be shallower during the winter months, producing a larger regional increase in response to rush hour traffic. The wintertime layer also expands and re-contracts earlier in the day than the summertime layer, resulting in both an earlier minimum and an earlier rise in afternoon–evening concentrations. An analysis of the regional signals calculated for similar periods in 2013 revealed qualitatively similar results (Fig. S1), although it should be noted that the 2013 analysis uses observations from a significantly different subset of sites in the BEACO$_2$N network.

We isolate the local signals by subtracting the network-wide regional component from the data record at each site. Median 1 min local CO_2 signals range from 0.3 to 40.2 ppm during the day (1100–1800 LT) and 1.1 to 38.5 ppm at night (2100–0400 LT) during the summer months, although the distributions are skewed, with the 10th to 90th percentile ranges stretching from -2.4 to 69.0 ppm during the day and -2.0 to 45.0 ppm at night. During the winter months, the daytime medians range from 3.6 ppm to 34.8 ppm (-7.0 to 90.8 ppm 10th to 90th percentile range) and -0.8 ppm to 58.7 ppm (-15.0 to 90.6 ppm 10th to 90th percentile range) at night. A full picture of the overall distributions is shown in Figs. S2 and S3, confirming a much greater frequency of high CO_2 concentrations during the winter months. In both seasons, the distribution of the local enhancements is typically unimodal with a heavy right-hand tail, although some sites exhibit more complex bi- or multi-modal distributions.

By definition, we expect these local signals to represent a unique combination of emission sources and atmospheric dynamics specific to a given site. Mobile sources are estimated to comprise approximately 40% of the San Francisco Bay Area's annual CO_2 emissions (Claire et al., 2015) and are likely to represent an even larger fraction within the urban core, where electricity and co-generation sources are less abundant. However, as noted in the discussion of the regional signals above, direct observation of the magnitude and variation of traffic emissions via ambient CO_2 concentrations is complicated by the coincident variation in turbulent mixing and boundary layer height as the earth's surface warms and cools at sunrise and sunset (Fig. S4).

In order to more directly examine the relationship between highway traffic flow and urban CO_2 concentrations, we begin by analyzing the subset of observations collected between 0400 and 0800 LT at the LAN site, located less than 40 m from Interstate 880. During this period, traffic emissions are high, but the boundary layer is relatively shallow, thus increasing the sensitivity of the surface-level monitor to the traffic signal. The resultant strong positive correlation between rush hour traffic flow and local CO_2 concentrations is shown in Fig. 5, along with the median CO_2 concentrations observed in each 500 veh h^{-1} traffic flow increment and the linear regressions through these binned medians. (An alternative analysis using traffic density–obtained by dividing the traffic flow by the average vehicle speed–yields almost identical results.) We observe a factor of 2 difference in local CO_2 between congested vs. free-flowing conditions, similar to that observed by a previous on-road mobile monitoring study by Maness et al. (2015). The uncertainty in the slope of the linear regression is 17%, indicating that

this analysis of a single site could be used to detect 17% changes in average emissions per vehicle. For reference, under the Corporate Average Fuel Economy standards, the state of California aims to achieve a fleet-wide average fuel economy of 54.5 miles per gallon by the year 2025 (US EPA, 2012), corresponding to a 35% decrease in emissions relative to the 35.5 miles per gallon economy of 2012–2016 model year vehicles.

In addition to this first-order sensitivity to vehicle emissions at the near-roadway LAN site, we find that policy-relevant emission changes can also be detected using nodes stationed greater distances from the highway by controlling for the impacts of dispersion. To do so, we decompose the CO_2 signals into terms that represent the influence of meteorology and emissions separately via a multiple linear regression approach analogous to that described by de Foy (2018). Briefly, linear coefficients describing the relationship of a site's CO_2 signal to temperature, specific humidity, wind, boundary layer height, time of day, day of week, and time of year are derived in an iterative, compounding fashion, with the variable leading to the greatest increase in the square of the Pearson correlation coefficient being added to the regression until the addition of a new variable no longer increases the r^2 value by at least 0.005. Temperature, specific humidity, wind speed, and wind direction are taken from the Port of Oakland International Airport weather station maintained by the NOAA Integrated Surface Database (https://www.ncdc.noaa.gov/isd/) and boundary layer heights are provided by the ECMWF's ERA-Interim model (Dee et al. 2011; http://apps.ecmwf.int/datasets/). The nonlinear relationship between CO_2 concentrations and wind or boundary layer height is captured by dividing these meteorological datasets into quartiles and deriving a linear coefficient for each subset. The wind speed quartiles are further subdivided by wind direction before fitting.

For this analysis, we use hourly total CO_2 concentrations (the sum of the local and regional components) measured at five sites between 15 February 2017 and 15 February 2018; a representative comparison of the observed and modeled results at the LCC site is shown in Fig. S5. The intercept of the multiple linear regression provides an estimate of the average background CO_2 concentration observed at a given site over the entire analysis period; here we find a mean intercept of 426 ppm across the five sites. This is considerably higher than the average 407 ppm regional signal calculated for the summer months using the bottom 10th percentile method described above, but in good agreement with the average wintertime regional signal (425 ppm).

Multiple linear regression coefficients are derived for each hour of the day during five types of days of the week (Mondays, Tuesdays through Thursdays, Fridays, Saturdays, and Sundays); for clarity, Fig. 6 shows the regression coefficients for Tuesdays through Thursdays and Sundays. These MLR "factors" signify the average CO_2 enhancement or depletion (in ppm) uniquely associated with a particular hour of a particular day of the week. The dependencies on time of day and day of week derived via this method primarily reflect the changes in emissions, as the influence of the coincident changes in atmospheric dynamics has been at least partially controlled for. Indeed, we do observe some intuitive patterns in the linear regression coefficients, such as higher coefficients on weekday mornings corresponding to higher rush hour traffic emissions on those days. As expected, the weekday enhancement is larger at the sites located close to a freeway (e.g. 520% at FTK) but is less pronounced at LBL (70%), which is farther away from major mobile sources. For reference, the 1 km by 1 km FIVE mobile emission inventory developed for the San Francisco Bay Area by McDonald et al. (2014) predicts a ~210% weekday

enhancement on average, peaking around 0500 LT, much earlier in the day than is observed here. When we examine the relationship between these multiple linear regression coefficients and morning traffic flow as we did at LAN (Fig. 7), we find positive correlations enabling the detection of 11–30% changes in emissions. This is sufficient sensitivity to detect and monitor future increases in the fuel efficiency of the California passenger vehicle fleet with a record as short as 2–3 years.

It is likely that even greater sensitivity could be achieved with more accurate meteorological datasets. While the single weather station and relatively coarse (0.125° by 0.125°) reanalysis product we use here may be adequate to represent the meteorological conditions across some domains, the San Francisco Bay Area is at the high end of complexity in terms of terrain and microclimatology. Higher resolution boundary layer heights and neighborhood-specific wind observations may improve the results of our multiple linear regression, but these types of measurements are rarely available on the spatial scale of the BEACO$_2$N instrument and are difficult to simulate with accuracy (Jiménez et al., 2013; Banks et al., 2016). In future work, high-density networks like BEACO$_2$N may therefore be useful not just in source attribution but also in providing a much needed observational constraint on our understanding of near-surface transport.

Future work will also make use of the ancillary datasets provided by the BEACO$_2$N platform, such as the concurrent NO_x and CO concentrations. The ratio of these species to CO_2 provides a unique signature for each different CO_2 source (e.g. Ban-Weiss et al., 2008; Harley et al., 2005), allowing "plumes" or other subsets of the data record to be directly attributed to specific (e.g. mobile) source types and allowing the relationship between these specific activities and CO_2 mixing ratios to be derived more precisely. With such a precise methodology for converting between emissions and concentrations, subtler interannual trends in emissions could be detected, for example changes in vehicle emissions following construction of new housing.

4 Conclusions

We have described the heterogeneity measured at the individual sites of a high-density, surface-level urban CO_2 monitoring network. Networkwide, correlation length scales are found to be slightly longer during daytime during the summer, and generally shorter during winter months, but falling in the range of values reported previously based on other stationary observation networks and mobile monitoring campaigns. High nearfield correlations are thought to be driven by shared sensitivity to local emission events, while moderate farfield correlations reflect regional episodes, suggesting that a given site's data record is likely a convolution of both phenomena. We therefore present a methodology for separating the observed CO_2 concentrations into local and regional components and observe distinct distributions (i.e. unimodal vs. bimodal) of local CO_2 enhancements within single neighborhoods. A clear relationship is seen between morning rush hour traffic counts and local CO_2 concentrations, allowing for the detection of changes in vehicle emissions within 2–3 years, if those changes proceed at a rate consistent with policy objectives.

Prior publications (e.g., McKain et al., 2012; Kort et al., 2013; Wu et al., 2018) have favored sparser networks of high-quality instruments, criticizing high-density, low-cost approaches as either: (a) providing redundant constraints on total urban emissions, (b) offering information on CO_2 sources in their immediate surroundings only, or (c) possessing insufficient accuracy to resolve small emission trends. The ideal trade-off between measurement quality and instrument quantity has been

investigated previously using an ensemble of observing system simulations by Turner et al. (2016), who found BEACO$_2$N-like observing systems to outperform smaller, higher quality networks in estimating regional as well as more localized emission phenomena. While Turner et al. saw significant benefits to achieving an instrument precision of 1 ppm, further increases in measurement quality offered little advantage in constraining emissions, especially those from line and point sources.

This work thus provides an important data-based verification of the conclusions of Turner et al.'s theoretical analysis. Not only do we demonstrate the ability of low-cost sensors to sufficiently constrain policy-relevant trends in line source (i.e. highway traffic) emissions, but we do so without the use of computationally intense and heavily parameterized atmospheric transport models. Furthermore, we show that a multiple linear regression analysis allows the signature of highway traffic to be extracted from sites located throughout the network, enabling trends in mobile emissions to be quantified without specially situated, roadside monitors. This is an important result, as deriving and implementing a particular, a priori network layout is a nontrivial task. Domain-specific transport patterns prevent the development of general principles of optimal sensor placement, and, even if ideal locations can be identified, cooperation from facilities in the area cannot be guaranteed. By establishing for the first time that an ad hoc, opportunistic sensor siting approach can nonetheless provide sensitivity to emission sources of interest, we thus improve the prospects for widespread adoption of distributed monitoring systems in the future.

Progress toward evaluating the capabilities and proper leverage of low-cost sensors has particular relevance for nations with rapidly developing economies, where CO_2 emissions are increasing much faster than the resources needed to monitor them by conventional means. Domestically, citizen science and environmental justice groups are also adopting these technologies (Snyder et al., 2013) as an economically accessible means of advocating for greater public health and ecological wellbeing. While the specific correlation lengths and emission estimates we derive here are unique to the San Francisco Bay Area domain, the sensor performance capabilities and data analysis techniques we outline provide guidance more generally to any future studies attempting to interpret similar datasets around the world. High-resolution surface networks enabled by low-cost technologies offer a unique opportunity to provide ground truth constraints on difficult to model near-surface dynamics as well as on the individual CO_2 sources and sinks that comprise the strategic backbone of greenhouse gas mitigation regulation.

5 Data Availability

All BEACO$_2$N CO_2 observations used in this analysis can be downloaded at doi:10.5281/zenodo.1206983. Traffic counts are available on the California Department of Transportation website (http://pems.dot.ca.gov/), wind, temperature, and humidity observations are available on the NOAA Integrated Surface Database website (http://www.ncdc.noaa.gov/isd/), and boundary layer heights are available on the ECMWF website (http://apps.ecmwf.int/datasets/).

Acknowledgements. This work was funded by the National Science Foundation (1035050; 1038191), the National Aeronautics and Aerospace Administration (NAS2-03144), the Bay Area Air Quality Management District (2013.145), and the Environmental Defense Fund. Additional support was provided by a NSF Graduate Research Fellowship to AAS, a Kwanjeong

Lee Chonghwan Educational Fellowship to JK, and a Hellman Fund Fellowship to KJL. We acknowledge the use of datasets maintained by the California Department of Transportation, the National Oceanic and Atmospheric Administration, as well as the European Centre for Medium-Range Weather Forecasts.

References

Banks, R. F., Tiana-Alsina, J., Baldasano, J. M., Rocadenbosch, F., Papayannis, A., Solomos, S., and Tzanis, C. G.: Sensitivity of boundary-layer variables to PBL schemes in the WRF model based on surface meteorological observations, lidar, and radiosondes during the HygrA-CD campaign, Atmos. Res., 176, 185–201, doi:10.1016/j.atmosres.2016.02.024, 2016.

Ban-Weiss, G. A., McLaughlin, J. P., Harley, R. A., Lunden, M. M., Kirchstetter, T. W., Kean, A. J., Strawa, A. W., Stevenson, E. D., and Kendall, G. R.: Long-term changes in emissions of nitrogen oxides and particulate matter from on-road gasoline and diesel vehicles, Atmos. Environ., 42, 220–232, doi:10.1016/j.atmosenv.2007.09.049, 2008.

Beckerman, B., Jerrett, M., Brook, J. R., Verma, D. K., Arain, M. A., and Finkelstein, M. M.: Correlation of nitrogen dioxide with other traffic pollutants near a major expressway, Atmos. Environ., 42, 275–290, doi:10.1016/j.atmosenv.2007.09.042, 2008.

Bréon, F. M., Broquet, G., Puygrenier, V., Chevallier, F., Xueref-Remy, I., Ramonet, M., Dieudonné, E., Lopez, M., Schmidt, M., Perrussel, O., and Ciais, P.: An attempt at estimating Paris area CO_2 emissions from atmospheric concentration measurements, Atmos. Chem. Phys., 15, 1707–1724, doi:10.5194/acp-15-1707-2015, 2015.

Brown, E. G.: 2016 ZEV action plan: an updated roadmap toward 1.5 million zero-emission vehicles on California roadways by 2025, Governor's Interagency Working Group on Zero-Emission Vehicles, Sacramento, CA, USA, 2016.

Chen, J., Viatte, C., Hedelius, J. K., Jones, T., Franklin, J. E., Parker, H., Gottlieb, E. W., Wennberg, P. O., Dubey, M. K., and Wofsy, S. C.: Differential column measurements using compact solar-tracking spectrometers, Atmos. Chem. Phys., 16, 8479–8498, doi:10.5194/acp-16-8479-2016, 2016.

Choi, W., Winer, A. M., and Paulson, S. E.: Factors controlling pollutant plume length downwind of major roadways in nocturnal surface inversions, Atmos. Chem. Phys., 14, 6925–6940, doi:10.5194/acp-14-6925-2014, 2014.

Claire, S. J., Dinh, T. M., Fanai, A. K., Nguyen, M. H., and Schultz, S. A.: Bay Area emissions inventory summary report: greenhouse gases, Tech. rep., Bay Area Air Quality Management District, San Francisco, CA, USA, 2015.

Dee, D. P., Uppala, S. M., Simmons, A. J., Berrisford, P., Poli, P., Kobayashi, S., Andrae, U., Balmaseda, M. A., Balsamo, G., Bauer, P., Bechtold, P., Beljaars, A. C. M., van de Berg, L., Bidlot, J., Bormann, N., Delsol, C., Dragani, R., Fuentes, M., Geer, A. J., Haimberger, L., Healy, S. B., Hersbach, H., Hólm, E. V., Isaksen, L., Kållberg, P., Köhler, M., Matricardi, M., McNally, A. P., Monge-Sanz, B. M., Morcrette, J.-J., Park, B.-K., Peubey, C., de Rosnay, P., Tavolato, C., Thépaut, J.-N., and Vitart, F.: The ERA-Interim reanalysis: configuration and performance of the data assimilation system, Q. J. Royal Meteorol. Soc., 137, 553–597, doi:10.1002/qj.828, 2011.

de Foy, B.: City-level variations in NO_x emissions derived from hourly monitoring data in Chicago, Atmos. Environ., 176, 128–139, doi:10.1016/j.atmosenv.2017.12.028, 2018.

Gurney, K. R., Razlivanov, I., Song, Y., Zhou, Y., Benes, B., and Abdul-Massih, M.: Quantification of fossil fuel CO_2 emissions on the building/street scale for a large U.S. city, Environ. Sci. Technol., 46, 12194–12202, doi:10.1021/es3011282, 2012.

Harley, R. A., Marr, L. C., Lehner, J. K., and Giddings, S., N.: Changes in motor vehicle emissions on diurnal to decadal time scales and effects on atmospheric composition, Environ. Sci. Technol., 39, 5356–5362, doi:10.1021/es048172+, 2005.

Jiménez, P. A., Dudhia, J., González-Rouco J. F., Montávez, J. P., García-Bustamante, E., Navarro, J., Vilà-Guerau de Arellano, J., and Muñoz-Roldán, A.: An evaluation of WRF's ability to reproduce the surface wind over complex terrain based on typical circulation patterns, J. Geophys. Res. Atmos., 118, 7651–7669, doi:10.1002/jgrd.50585, 2013.

Kim, J., Shusterman, A. A., Lieschke, K. J., Newman, C., and Cohen, R. C.: The BErkeley Atmospheric CO_2 Observation Network: field calibration and evaluation of low-cost air quality sensors, Atmos. Meas. Tech. Discuss., in review, 2017.

Kort, E. A., Angevine, W. M., Duren, R., and Miller, C. E.: Surface observations for monitoring urban fossil fuel CO_2 emissions: minimum site location requirements for the Los Angeles Megacity, J. Geophys. Res. Atmos., 118, 1577–1584, doi:10.1002/jgrd.50135, 2013.

Maness, H. L., Thurlow, M. E., McDonald, B. C., and Harley, R. A.: Estimates of CO_2 traffic emissions from mobile concentration estimates, J. Geophys. Res. Atmos., 120, 2087–2102, doi:10.1002/2014jd022876, 2015.

McDonald, B. C., McBride, Z. C., Martin, E. W., and Harley, R. A.: High-resolution mapping of motor vehicle carbon dioxide emissions, J. Geophys. Res. Atmos., 119, 5283–5298, doi:10.1002/2013jd021219, 2014.

McKain, K., Wofsy, S. C., Nehrkorn, T., Eluszkiewicz, J., Ehleringer, J. R., and Stephens, B. B.: Assessment of ground-based atmospheric observations for verification of greenhouse gas emissions from an urban region, P. Natl. Acad. Sci. USA, 109, 8423–8428, doi:10.1073/pnas.1116645109, 2012.

McKain, K., Down, A., Raciti, S. M., Budney, J., Hutrya, L. R., Floerchinger, C., Herndon, S. C., Nehrkorn, T., Zahniser, M. S., Jackson, R. B., Phillips, N., and Wofsy, S. C.: Methane emissions from natural gas infrastructure and use in the urban region of Boston, Massachusetts, P. Natl. Acad. Sci. USA, 112, 1941–1946, doi:10.1073/pnas.1416261112, 2015.

Newman, S., Xu, X., Gurney, K. R., Hsu, Y. K., Li, K. F., Jiang, X., Keeling, R., Feng, S., O'Keeffe, D., Patarasuk, R., Wong, K. W., Rao, P., Fischer, M. L., and Yung, Y. L.: Toward consistency between trends in bottom-up CO_2 emissions and top-down atmospheric measurements in the Los Angeles megacity, Atmos. Chem. Phys., 16, 3843–3863, doi:10.5194/acp-16-3843-2016, 2016.

Pacala, S. W., Breidenich, C., Brewer, P. G., Fung, I., Gunson, M. R., Heddle, G., Law, B., Marland, G., Paustian, K., Prather, M., Randerson, J. T., Tans, P., and Wofsy, S. C.: Verifying Greenhouse Gas Emissions: Methods to Support International Climate Agreements, The National Academies Press, Washington, D. C., 2010.

Patarasuk, R., Gurney, K. R., O'Keeffe, D., Song, Y., Huang, J., Preeti, R., Buchert, M., Lin, J. C., Mendoza, D., and Ehleringer, J. R.: Urban high-resolution fossil fuel CO_2 emissions quantification and exploration of emission drivers for potential policy applications, Urban Ecosyst., 19, 1013–1039, doi:10.1007/s11252-016-0553-1, 2016.

Pugliese, S. C., Murphy, J. G., Vogel, F. R., Moran, M. D., Zhang, J., Zheng, Q., Stroud, C. A., Ren, S., Worthy, D., and Broquet, G.: High-resolution quantification of atmospheric CO_2 mixing ratios in the Greater Toronto Area, Canada, Atmos. Chem. Phys., 18, 3387–3401, doi:10.5194/acp-18-3387-2018, 2017.

Shusterman, A. A., Teige, V. E., Turner, A. J., Newman, C., Kim, J., and Cohen, R. C.: The BErkeley Atmospheric CO_2 Observation Network: initial evaluation, Atmos. Chem. Phys., 16, 13449–13463, doi:10.5194/acp-16-13449-2016, 2016.

Turnbull, J. C., Sweeney, C., Karion, A., Newberger, T., Lehman, S. J., Tans, P. P., Davis, K. J., Lauvaux, T., Miles, N. L., Richardson, S. J., Cambaliza, M. O., Shepson, P. B., Gurney, K., Patarasuk, R., and Razlivanov, I.: Toward quantification and source sector identification of fossil fuel CO_2 emissions from an urban area: Results from the INFLUX experiment, J. Geophys. Res. Atmos., 120, 292–312, doi:10.1002/2014jd022555, 2015.

Snyder, E. G., Watkins, T. H., Solomon, P. A., Thoma, E. D. Williams, R. W., Hagler, G. S. W., Shelow, D., Hindin, D. A., Kilaru, V. J., and Preuss, P. W.: The changing paradigm of air pollution monitoring, Environ. Sci. Technol., 47, 11369–11377, doi:10.1021/es4022602, 2013.

Turner, A. J., Shusterman, A. A., McDonald, B. C., Teige, V., Harley, R. A., and Cohen. R. C.: Network design for quantifying urban CO_2 emissions: assessing trade-offs between precision and network density, Atmos. Chem. Phys., 16, 13465–13475, doi:10.5194/acp-16-13465-2016, 2016.

United Nations, Human Settlement Programme: Hot Cities: Battle-Ground for Climate Change, 2011.

United Nations, Framework Convention on Climate Change: Adoption of the Paris Agreement, 21st Conference of the Parties, Paris, 2015.

United States Environmental Protection Agency, 2017 and Later Model Year Light-Duty Vehicle Greenhouse Gas Emissions and Corporate Average Fuel Economy Standards, Washington, D.C., 2012.

Verhulst, K. R., Karion, A., Kim, J., Salameh, P. K., Keeling, R. F., Newman, S., Miller, J., Sloop, C., Pongetti, T., Rao P., Wong, C., Hopkins, F. M., Yadav, V., Weiss, R. F., Duren, R. M., and Miller, C. E.: Carbon dioxide and methane measurements from the Los Angeles Megacity Carbon Project – Part 1: calibration, urban enhancements, and uncertainty estimates, Atmos. Chem. Phys., 17, 8313–8341, doi:10.5194/acp-17-8313-2017, 2017.

Wu, K., Lauvaux, T., Davis, K. J., Deng, A., Lopez Coto, I., Gurney, K. R., and Patarasuk, R.: Joint inverse estimation of fossil fuel and biogenic CO_2 fluxes in an urban environment: An observing system simulation experiment to assess the impact of multiple uncertainties, Elem. Sci. Anth., 6, doi:10.1525/elementa.138, 2018.

Zhu, Y., Kuhn, T., Mayo, P., and Hinds, W. C.: Comparison of daytime and nighttime concentration profiles and size distributions of ultrafine particles near a major highway, Environ. Sci. Technol., 40, 2531–2536, doi:10.1021/es0516514, 2006.

Atmos. Chem. Phys. Discuss., https://doi.org/10.5194/acp-2018-344
Manuscript under review for journal Atmos. Chem. Phys.
Discussion started: 22 May 2018

Atmospheric Chemistry and Physics Discussions

Figure 1. Map of BEACO$_2$N node locations (black dots). Nodes used in this study are labeled. Map data © 2017 Google.

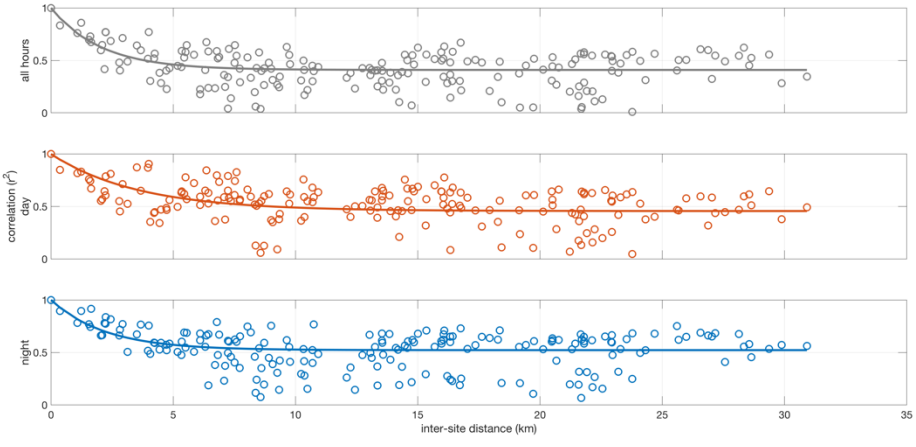

Figure 2. Optimal correlation coefficients for every possible pairing of summer 2017 sites as a function of their separation distance during all hours (top), daytime hours (1100–1800 LT, middle), and nighttime hours (2100–0400 LT, bottom). Solid lines show exponential decay of the correlation coefficients.

Atmos. Chem. Phys. Discuss., https://doi.org/10.5194/acp-2018-344
Manuscript under review for journal Atmos. Chem. Phys.
Discussion started: 22 May 2018

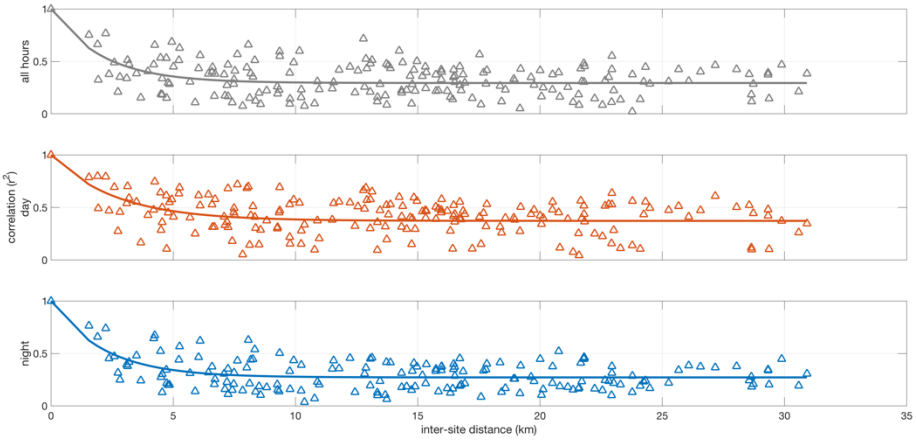

Figure 3. Optimal correlation coefficients for every possible pairing of winter 2017 sites as a function of their separation distance during all hours (top), daytime hours (1100–1800 LT, middle), and nighttime hours (2100–0400 LT, bottom). Solid lines show exponential decay of the correlation coefficients.

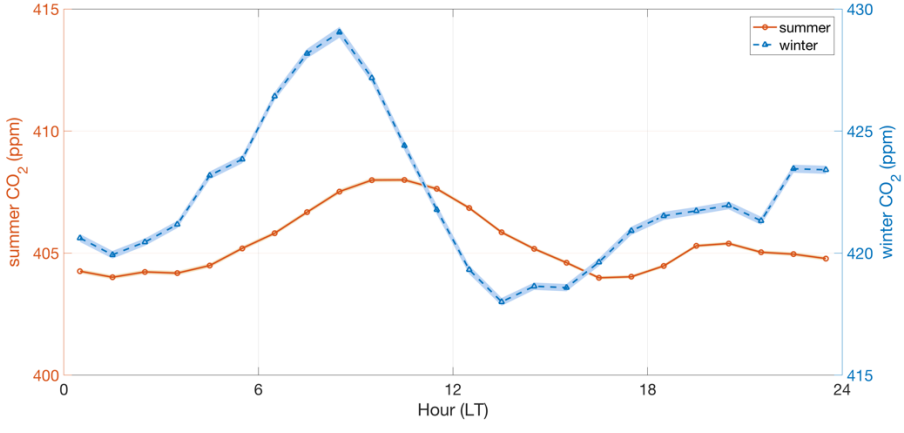

Figure 4. Hourly median values of the network-wide, regional CO_2 signals calculated for summer (orange) and winter (blue) periods in 2017. Lighter colored curves indicate the standard error; note the difference in y-scale.

Atmos. Chem. Phys. Discuss., https://doi.org/10.5194/acp-2018-344
Manuscript under review for journal Atmos. Chem. Phys.
Discussion started: 22 May 2018

Atmospheric Chemistry and Physics Discussions

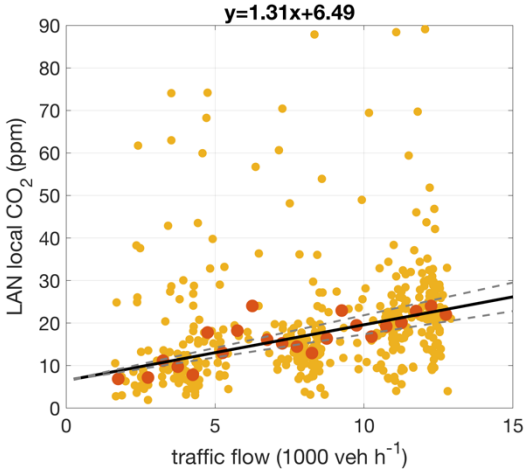

Figure 5. Morning (0400–0800 LT) local summertime CO_2 concentrations at LAN shown as a function of nearby highway traffic flow. Darker points indicate the median CO_2 concentration observed in each 500 veh h^{-1} traffic flow increment; black solid line indicates the linear regression through the binned medians (equation given above plot) and gray dashed lines show the uncertainty in the regression slope.

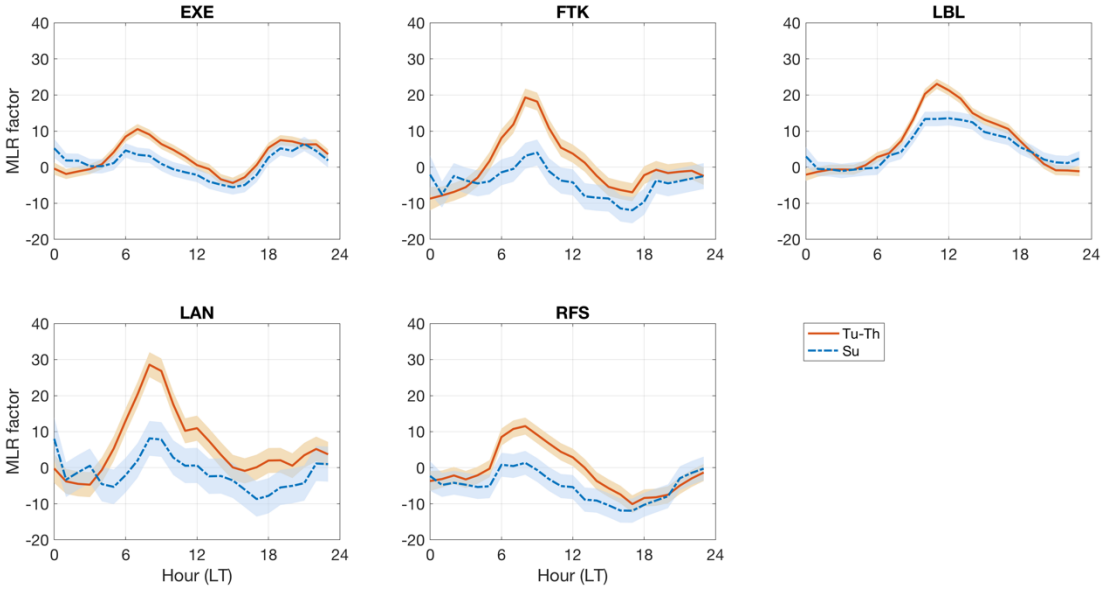

Figure 6. Multiple linear regression coefficients for five sites derived for each hour of the day on Tuesdays through Thursdays (orange solid line) and Sundays (blue dashed line) between 15 February 2017 and 15 February 2018.

Atmos. Chem. Phys. Discuss., https://doi.org/10.5194/acp-2018-344
Manuscript under review for journal Atmos. Chem. Phys.
Discussion started: 22 May 2018

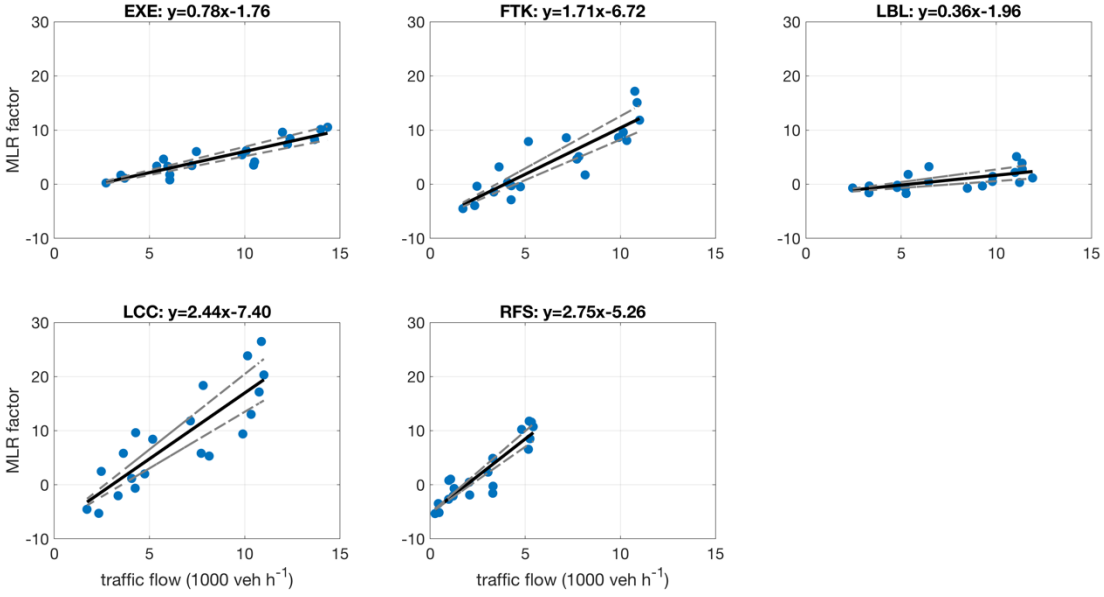

Figure 7. Morning (0400–0800 LT) multiple linear regression coefficients shown as a function of summertime traffic flow; black solid lines indicate the linear regression through the binned medians (equations given above each subplot) and gray dashed lines show the uncertainty in the regression slope.

Atmos. Chem. Phys. Discuss., https://doi.org/10.5194/acp-2018-344
Manuscript under review for journal Atmos. Chem. Phys.
Discussion started: 22 May 2018

Atmospheric Chemistry and Physics Discussions

SITE CODE	LAT (° N)	LON (° E)	TRAFFIC MONITOR IDs	DISTANCE FROM HIGHWAY (m)
ALB*	37.896	-122.292	401052, 402062	1390
BAM	37.788	-122.391	402815, 404920	170
BOD*	37.754	-122.156	401857, 401858	300
CHA	37.819	-122.181	400302, 400308	1720
COL	38.002	-122.289	401230, 401269	510
CPS*	37.848	-122.240	402201, 402202	220
DEJ†	37.933	-122.338	400361, 400445	950
EXB†	37.802	-122.397	402815, 404920	1570
EXE	37.801	-122.399	402815, 404920	1580
FTK	37.737	-122.173	JJAS: 400442, 400955 NDJ: 400608, 400793	1350
HRS*	37.809	-122.205	400302, 400308	700
LAN†	37.794	-122.263	400835, 408138	40
LBL	37.876	-122.252	400176, 400728	3090
LCC	37.736	-122.196	JJAS: 400442, 400955 NDJ: 400608, 400793	220
MAD†	37.928	-122.299	400819, 401558	1850
MAR†	37.863	-122.314	400176, 400728	950
MTA	37.995	-122.335	400538, 400976	2040
NOC*	37.833	-122.276	401211, 401513	750
NYS†	37.928	-122.359	400359, 400734	380
OHS*	37.804	-122.236	400261, 401017	160
PDS*	37.831	-122.257	400224, 401381	800
PER	37.943	-122.365	400639, 400738	1790
PTL	37.920	-122.306	400819, 401588	970
RFS	37.913	-122.336	400202, 400675	760
RHS†	37.953	-122.347	401228, 406660	1530
SHL	37.967	-122.298	416774, 416790	2030
SPB*	37.960	-122.357	401894, 401895	2280
STW†	37.990	-122.291	400313, 400902	500

Table 1: List of site geo-coordinates, relevant traffic monitor IDs, and approximate distance from a highway. Asterisks indicate sites with data available in winter 2017 only; daggers indicate sites with data available in summer 2017 only.